



Original Article

## Improving corrosion properties of manganese aluminium bronze alloys (MAB-Cu4) through electroless nickel phosphorus coating

Yasemin YILDIRAN AVCU\*<sup>id</sup>

Department of Mechanical Engineering, Kocaeli University, Kocaeli, Türkiye

### ARTICLE INFO

#### Article history

Received: 08 May 2024

Revised: 24 May 2024

Accepted: 01 June 2024

#### Key words:

Bronze alloys, corrosion, electroless coatings, nickel-phosphorus, structural properties.

### ABSTRACT

The objective of this study is to investigate how electroless nickel-phosphorus-coated Manganese Aluminum Bronze (MAB-CU4) alloys react to corrosion in a 0.5 M NaCl environment. Scanning electron microscopy examinations revealed that the coating layer has a cauliflower-like structure, and there are some porosities within the coating from the release of H<sub>2</sub> gas during the coating's deposition. EDS analysis detected only Ni and P on the coating, while XRD analysis indicated that the coating has an amorphous and nanocrystalline structure. Electrochemical corrosion tests showed that the untreated MAB-Cu4 alloy's E<sub>corr</sub> value dropped to -0.47 V in 1000 seconds and then stabilized. Within 200 seconds, the Ni-P-coated MAB-Cu4 alloy's corrosion potential dropped to -0.425 V from -0.412 V. Then, a progressive increase brought the potential value to -0.395V around the 2000<sup>th</sup> second. Upon examination of the anodic polarisation curve for the Ni-P-coated MAB-Cu4 alloy, it was found that the E<sub>corr</sub> value was lower than that of the untreated alloy (-0.532 V). The Ni-P-coated sample exhibits higher intensity values at low and medium frequencies compared to the untreated sample, indicating that the corrosion mechanism is identical for both samples; however, the Ni-P-coated sample exhibits superior corrosion resistance. Considering the frequent exposure of MAB alloys to corrosive environments, the implementation of an electroless nickel phosphorus coating may potentially improve their resistance to corrosion and extend their operational lifespan.

**Cite this article as:** Yıldıran Avcu, Y. (2024). Improving corrosion properties of manganese aluminium bronze alloys (MAB-Cu4) through electroless nickel phosphorus coating. *J Adv Manuf Eng*, 5(1), 15–20.

### INTRODUCTION

Developments in ship materials are crucial for ensuring coastal defence security and enhancing maritime trade [1]. The propeller is the main propulsion mechanism of a marine vehicle, revolving at high speeds in saltwater, operating under conditions of prolonged immersion and high-speed rotation in seawater [2]. Thus, severe corrosion develops on the marine ship propeller [3]. Manganese aluminium bronze alloys (MAB) are commonly used copper alloys for producing maritime components, particularly large-sized

and high-speed ship propellers [1] due to their excellent casting capabilities, mechanical properties, corrosion resistance, tribological properties, and cavitation resistance [3–5]. Moreover, marine hydraulic components like pumps, valves, turbines, and rudders also utilize MAB alloys, which can be utilised under corrosive conditions.

MAB alloys include substantial proportions of Ni, Al, Mn, and Fe. Cast MAB alloys are mostly composed of a coarse  $\alpha$  phase, an ordered solid solution  $\beta$  phase with an irregular form, and large  $\kappa$  phases, which are Fe and Mn-rich intermetallic compounds [5]. The complex microstructure

\*Corresponding author.

\*E-mail address: [yasemin.yildiran@kocaeli.edu.tr](mailto:yasemin.yildiran@kocaeli.edu.tr)



of these alloys is influenced by its chemical composition and processing methods [4], including heat treatments, which negatively impact their resistance to corrosion in saltwater [5]. Their multi-phase microstructure often undergoes selective phase corrosion due to the difference in chemical content and crystal structure among various phases, leading to galvanic corrosion [1]. Their corrosion behaviour varies depending on the pH level and the kind and amount of aggressive ions present in the corrosive environment [1]. Recently, the corrosion behaviour of MAB alloys has been extensively researched [1–8] yet there is a notable need to enhance their corrosion resistance. Electroless coatings may promise in enhancing their resistance to corrosion, but further study is required.

Electroless coatings can produce uniform deposits, especially on complicated components [9]. Thus, electroless nickel plating is a commonly employed technique for coating copper and its alloys. An external power source is unnecessary for this process, as the reactions occur autocatalytically. The coating layer exhibits a uniform thickness distribution across the entire surface of the parts. The primary objective of using this material is to achieve exceptional resistance to corrosion and abrasion. Additionally, it possesses advantageous characteristics such as high brightness, rapid deposition rate, and excellent solderability. Particularly, electroless Ni-P coatings show significant potential for improving the corrosion resistance of copper alloys [9–11], where the deposition of the coating is relatively flexible and is one of the surface treatment technologies widely used in industries [10]. They offer corrosion protection by establishing a barrier between the underlying material and the environment that causes corrosion. Ni-based electroless coatings with outstanding engineering features are growing in the aerospace, military, automotive, oil, gas, and marine sectors [11].

The corrosion resistance of Ni-P coatings is influenced by the phosphorus ratio, internal stress, and amorphism ratio [12]. Liu et al. [10] employed a Ni-P/Ni-B duplex coating layer to the CuSn10Pb10 alloy resulted in enhanced surface antifriction and wear resistance. The Ni-P coating layer acts as a barrier, preventing the CuSn10Pb10 alloy from dissolving in the Ni-B plating bath and allowing the Ni-B layer to be deposited [10]. To the author's knowledge, there is no study using Ni-P coatings to enhance the corrosion resistance of bronze alloys used in the marine atmosphere. In the present study, manganese aluminium bronze (MAB-Cu4), a bronze commonly used in propellers, was coated with electroless Ni-P, and its corrosion properties were examined in a 0.5 M NaCl environment.

## MATERIALS AND METHODS

Cylindrical geometry samples with a diameter of 20 mm and a height of 10 mm were prepared from the MAB alloy produced by the casting method for coating and characterization processes. The surfaces of the samples were grinded using 180–400–600–800–1200 grid sandpapers, respectively, and were made suitable for the coating process. The dirt and grease formed on the sample surface during processing were

ultrasonically cleaned using acetone and ethanol, respectively, for 10 minutes each. Sensitization and activation processes were applied to the surfaces before coating. To obtain a clean and active surface after ultrasonic cleaning, the samples were immersed in silver nitrate solution (5 g/l AgNO<sub>3</sub>) and sodium boron hydride solution (2 g/l NaBH<sub>4</sub> and 10 g/l NaOH) for 60 seconds and at room temperature, respectively.

The plating process was carried out in an alkaline Ni-P bath. In process, NiSO<sub>4</sub>·6H<sub>2</sub>O was used as a nickel source, NaH<sub>2</sub>PO<sub>2</sub>·H<sub>2</sub>O as a reducing agent, Na<sub>3</sub>C<sub>6</sub>H<sub>5</sub>O<sub>7</sub> as a complexing agent, CH<sub>4</sub>N<sub>2</sub>S as a stabilizer, and NaOH as a pH adjuster. The bath composition is given in Table 1 and the bath preparation procedure can be found elsewhere [10]. After the procedure, the samples were taken from the bath and cleaned with boiling water twice.

The morphology of the coated sample surfaces was examined by scanning electron microscopy (SEM, JEOL 6060 LV). The chemical composition of the coating was examined using energy dispersive X-ray spectroscopy (EDS) integrated with SEM. The phases in the structure were analyzed by X-ray diffraction (XRD, Rigaku D/Max 2200). Details of the XRD analysis can be found elsewhere [13]. The electrochemical corrosion properties of both uncoated and Ni-P coated MAB-Cu4 were examined using potentiodynamic polarization (PP) and electrochemical impedance spectroscopy (EIS) methods. Aqueous 0.5 M NaCl solution was chosen as the corrosive medium for the experiments. A three-electrode cell (Gamry Paracell, USA) was used for the tests; working, counter and reference electrodes are sample, graphite and calomel, respectively. The samples are 10×10 mm in size and the area exposed to the corrosive medium is 0.28 mm<sup>2</sup>. Before each experiment, open circuit potential (OCP) measurements were carried out for 60 minutes until the corrosion potential reached a steady state. Potentiodynamic polarization measurements were carried out in the ± 1.0 V potential range and at a scan rate of 1 mV/s. Tafel extrapolation was applied to PP curves via the Gamry Echem software and the corrosion rate was determined. EIS measurements were performed using 10 mV AC perturbation and 10 points/decade parameters, and the frequency range is 10<sup>-2</sup>–10<sup>5</sup> Hz. Finally, the micrographs of the cross-sectional microstructures of untreated-MAB-CU4 (a) and coated-MAB-CU4 alloy (b) after corrosion tests were examined via optical microscopy (Nikon Eclipse L 150).

**Table 1.** Bath composition and parameters of the Ni-P coating process

Component/parameter	Value
NiSO <sub>4</sub> ·6H <sub>2</sub> O	25 g/l
NaH <sub>2</sub> PO <sub>2</sub> ·H <sub>2</sub> O	20 g/l
Na <sub>3</sub> C <sub>6</sub> H <sub>5</sub> O <sub>7</sub>	20 g/l
CH <sub>4</sub> N <sub>2</sub> S	5 mg/l
NaOH	5 g/l
pH	10±0.2
Temperature	90°C
Time	60 min.

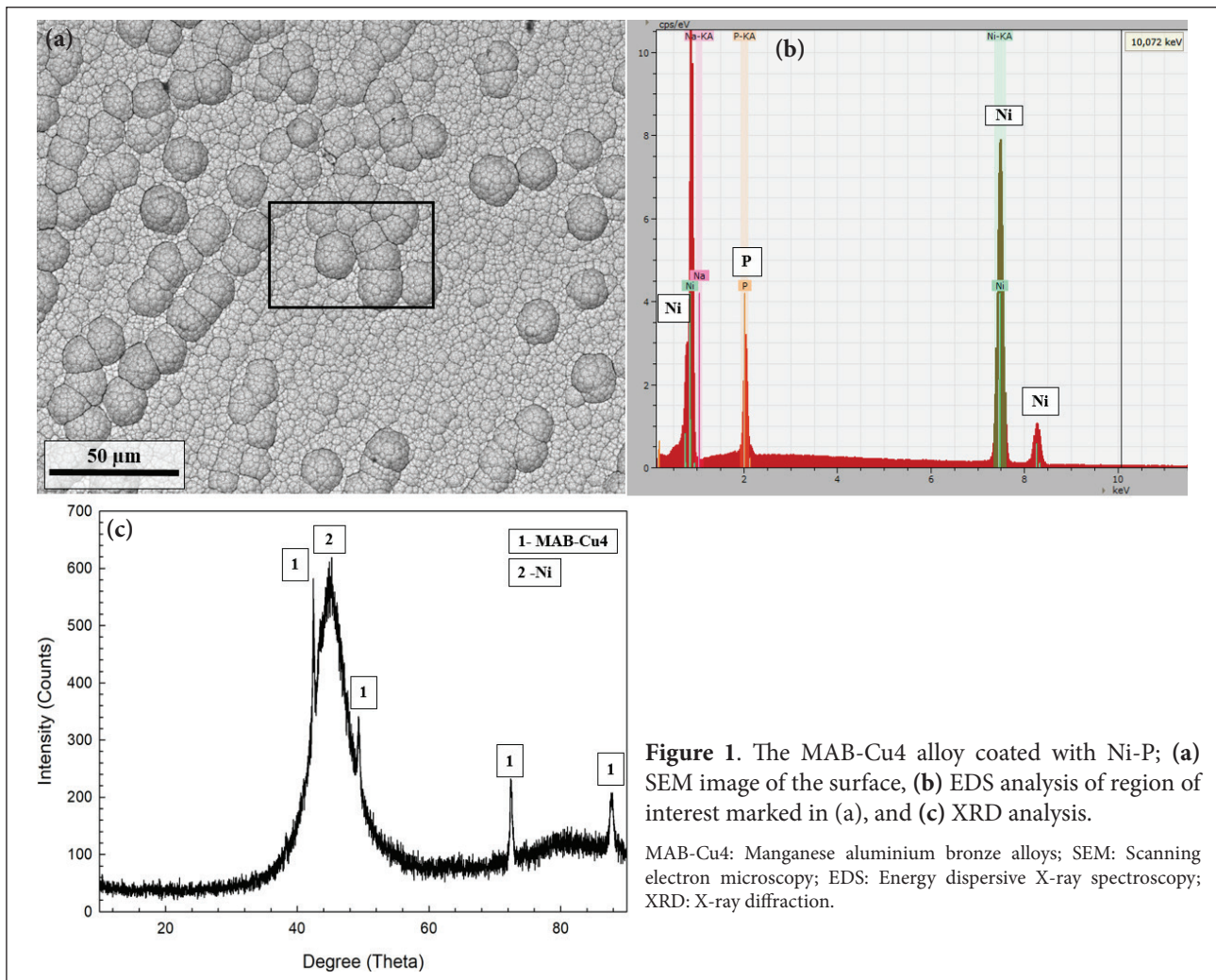


**Figure 1.** The MAB-Cu4 alloy coated with Ni-P; (a) SEM image of the surface, (b) EDS analysis of region of interest marked in (a), and (c) XRD analysis.

MAB-Cu4: Manganese aluminium bronze alloys; SEM: Scanning electron microscopy; EDS: Energy dispersive X-ray spectroscopy; XRD: X-ray diffraction.

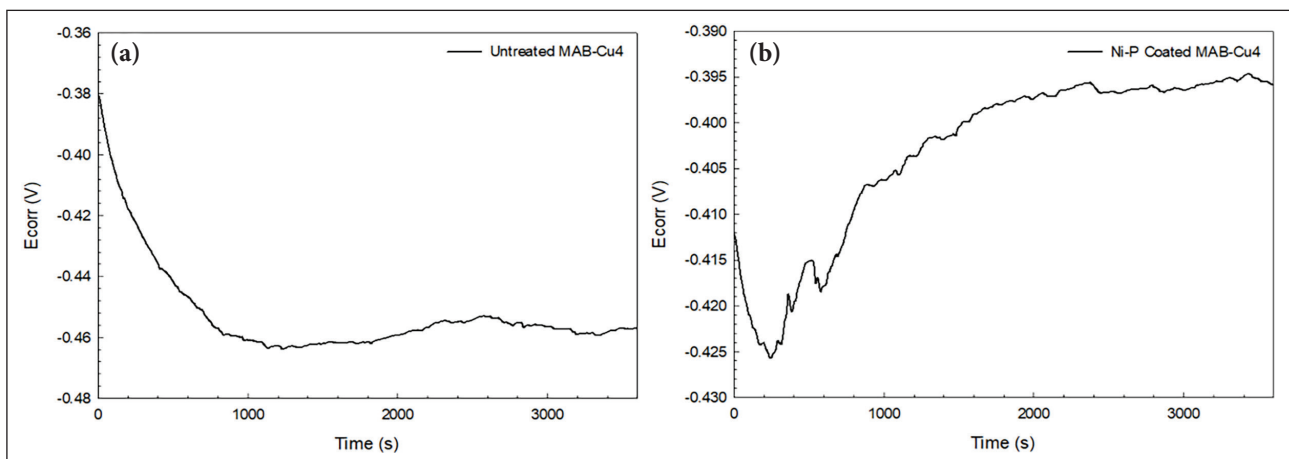


**Figure 2.** Corrosion potential-time graphs obtained in aqueous 0.5 M NaCl environment for (a) untreated and (b) Ni-P coated MAB-Cu4 alloys.

MAB-Cu4: Manganese aluminium bronze alloys.

## RESULTS AND DISCUSSION

Figure 1a depicts the surface image of the Ni-P-coated MAB-Cu4 alloy, in which there is evidence of the accumulation of a coating layer on the entire surface of the alloy. The coating layer possesses a cauliflower-like structure

and exhibits the same characteristics as those identified in previous studies [14]. On the surface, randomly distributed cluster formations resulting from Ni-P grain aggregation are visible. Besides, porosity formation is relevant in certain regions within the coating layer, resulting from the release of H<sub>2</sub> gas during the deposition of the coating.

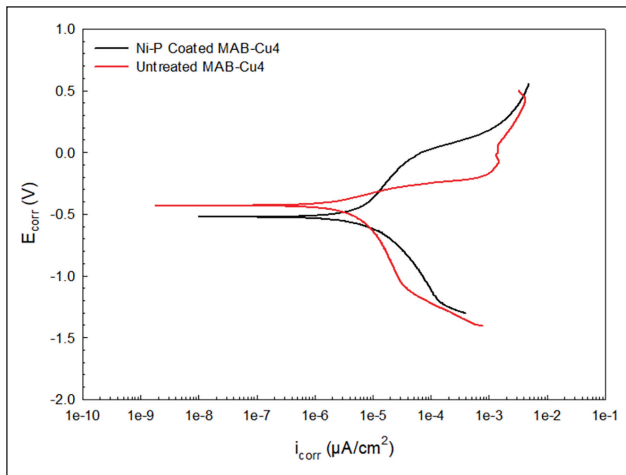


**Figure 3.** Potentiodynamic polarization curves of untreated and Ni-P coated MAB-Cu4 alloys obtained in aqueous 0.5 M NaCl corrosive environment.

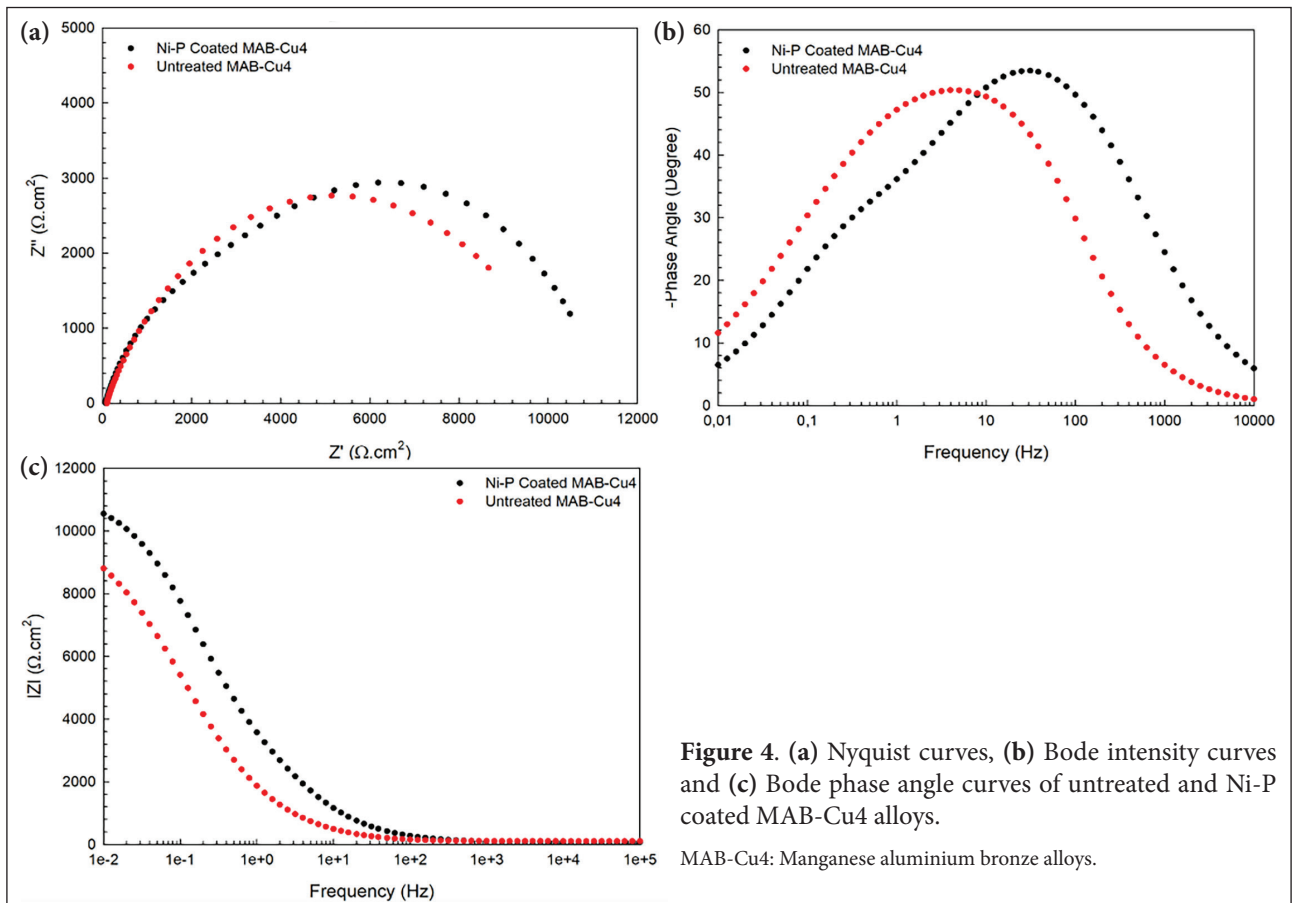
EDS analysis (Fig. 1b) performed on the region of interest shown in the inlet image in Figure 1a reveals the presence of Ni, P, and elements throughout the surface. The XRD analysis (Fig. 1c) suggests that the coating possesses an amorphous and nanocrystalline composition, while typical peaks of electroless nickel coatings are detected [15, 16]. In addition, four additional peaks were identified, which correspond to the substrate material MAB-Cu4 alloy.

Figure 2 displays the corrosion potential ( $E_{corr}$ ) over time for both the untreated and Ni-P-coated MAB-Cu4 al-

loy samples, obtained from electrochemical corrosion tests conducted in a 0.5 M NaCl aqueous environment. The untreated MAB-Cu4 alloy's  $E_{corr}$  value, initially around -0.30 V, decreased to approximately -0.47 V within a span of approximately 1000 seconds. Subsequently, consistent and steady behaviour was observed throughout the entire corrosion test, which lasted for 3600 seconds. The corrosion potential of the Ni-P-coated MAB-Cu4 alloy, initially around -0.412 V, decreased within the first 200 seconds and reached approximately -0.425 V. Subsequently, there was a progressive increasing trend, leading to a potential value of -0.395V around the 2000<sup>th</sup> second. This was followed by a period of consistent values until the conclusion of the measurement. During this period of growth, there were minor drops in potential observed around the 400<sup>th</sup> and 500<sup>th</sup> seconds.

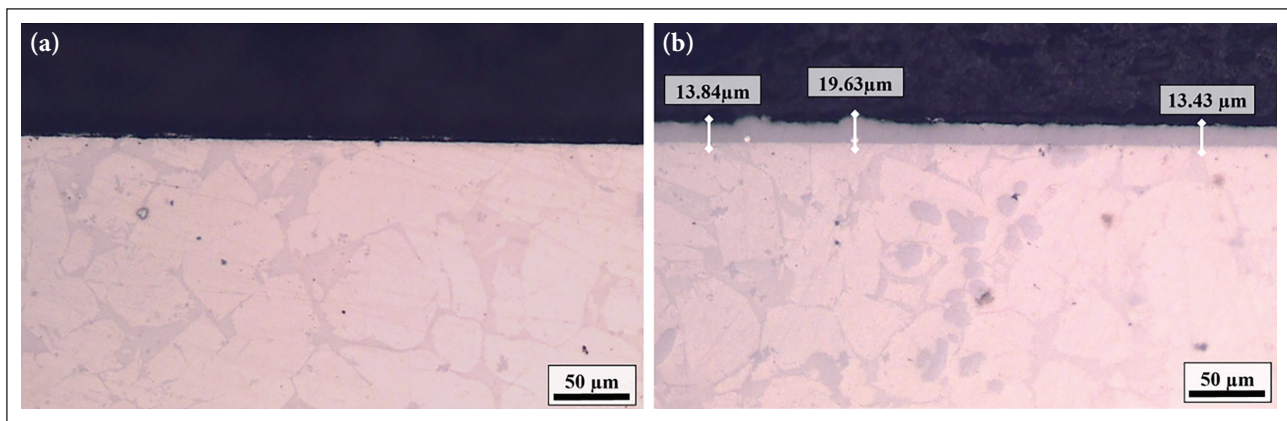
Figure 3 gives the potentiodynamic polarization curves of the untreated and Ni-P-coated samples. The corrosion potential ( $E_{corr}$ ) was determined to be -0.43 V. At a voltage of around -0.08 V, the alloy began to exhibit a tendency to passivation, resulting in a corrosion current density ( $i_{corr}$ ) of 0.013 A/cm<sup>2</sup> at a corrosion potential of -0.013 V. Transpassivation took place at an  $E_{corr}$  value of around 0.02 V, with the  $E_{corr}$  value measuring 0.014 A/cm<sup>2</sup>. Upon examination of the anodic polarization curve for the Ni-P coated MAB-Cu4 alloy, it was found that the  $E_{corr}$  value was lower than that of the untreated alloy (-0.532 V). Furthermore, passivation was not detectable.

Figure 4 displays the results of an electrochemical impedance spectroscopy (EIS) test that was done on



**Figure 4.** (a) Nyquist curves, (b) Bode intensity curves and (c) Bode phase angle curves of untreated and Ni-P coated MAB-Cu4 alloys.

MAB-Cu4: Manganese aluminium bronze alloys.



**Figure 5.** Optical microscope micrographs of the cross-sectional microstructures of untreated-MAB-CU4 (a) and coated-MAB-CU4 alloy (b) after corrosion tests.

untreated and Ni-P-coated MAB-Cu4 alloys in a 0.5 M NaCl solution that is corrosive. Figure 4a clearly demonstrates that each material's curves consist of a single semicircular arc, which indicates that charge-controlled dissolution solely influences the dissolution of the relevant material. The arc diameter also serves as an indicator of the level of resistance to corrosion. Previous research suggests that an increase in the arc's diameter leads to a greater level of corrosion resistance [17]. Therefore, the larger arc diameter of the Ni-P-coated MAB-Cu4 alloy leads to greater corrosion resistance. Examining the Bode intensity curve graphs provided in Fig. 4b reveals a high degree of similarity between the curves for both samples. Nevertheless, the Ni-P-coated sample exhibits higher intensity values at low and medium frequencies compared to the untreated sample. This indicates that the corrosion mechanism is identical for both samples; however, the Ni-P-coated sample exhibits superior corrosion resistance. In Bode phase angle curves (Fig. 4c), the presence of a single peak in these curves shows that corrosion is occurring because of a single reaction, which is occurring at the same time as the results of the Nyquist and Bode intensity curves. The Ni-P-coated sample exhibits a peak at higher phase angle values and higher frequency values, suggesting a higher level of corrosion resistance.

Figure 5 displays the optical microscope images of the cross-sectional microstructures of the untreated and coated MAB-CU4 alloy following corrosion tests. The protective layer and coating layer do not show a clear interaction, but the coating layer shows a clear adhesion with the substrate. The coating also maintains its integrity after the corrosion tests since a uniform coating layer with a thickness between 13 and 20  $\mu\text{m}$  is visible in Figure 5b.

## CONCLUSION

This study examines the corrosion properties of electroless nickel-phosphorus-coated manganese aluminium bronze (MAB-CU4) alloys in a 0.5 M NaCl solution.

The coating layer exhibits a cauliflower-like structure

with porosities resulting from the release of  $\text{H}_2$  gas during deposition. EDS analysis detected Ni, P, and various elements on the coating, while XRD analysis indicated that the coating has an amorphous and nanocrystalline structure. Electrochemical corrosion tests revealed that the  $E_{\text{corr}}$  value of the untreated MAB-Cu4 alloy decreased to  $-0.47$  V within 1000 seconds. Then, a pattern of reliable and unwavering conduct was observed. After 200 seconds, the corrosion potential of the Ni-P-coated MAB-Cu4 alloy decreased from  $-0.412$  V to  $-0.425$  V. Then, there was a gradual rise in the potential value, reaching  $-0.395$  V at approximately the 2000<sup>th</sup> second. The anodic polarisation curve analysis of the Ni-P-coated MAB-Cu4 alloy revealed that the  $E_{\text{corr}}$  value was lower than that of the untreated alloy ( $-0.532$  V). The Ni-P-coated sample shows higher intensity values at low and medium frequencies compared to the untreated sample, suggesting a similar corrosion mechanism for both samples. However, the Ni-P-coated sample demonstrates better corrosion resistance. Electroless nickel phosphorus coating on MAB alloys could increase their corrosion resistance and lifespan, especially in corrosive environments. Future research investigating their resistance to cavitation erosion is essential to enhance their application as marine propellers.

## Data Availability Statement

The author confirm that the data that supports the findings of this study are available within the article. Raw data that support the finding of this study are available from the corresponding author, upon reasonable request.

## Conflict of Interest

The author declared no potential conflicts of interest with respect to the research, authorship, and/or publication of this article.

## Use of AI for Writing Assistance

Not declared.

## Ethics

There are no ethical issues with the publication of this manuscript.

## REFERENCES

- [1] Song, Q.-n., Li, H.-l., Xu, N., Jiang, Z.-y., Zhang, G.-y., Bao, Y.-f., . . . & Qiao, Y.-x. (2023). Selective phase corrosion and cavitation erosion behaviors of various copper alloys in 3.5% NaCl solutions with different pH values. *Transactions of Nonferrous Metals Society of China*, 33(10), 3039–3053. [\[CrossRef\]](#)
- [2] Song, Q. N., Wang, Y., Wu, Y. Q., Zhu, X. Y., Xu, N., Zhang, G. Y., . . . & Qiao, Y. X. (2023). Effect of pre-corrosion on the cavitation erosion performance of two aluminum bronzes in 3.5% NaCl solution. *Materials Today Communications*, 37, Article 107265. [\[CrossRef\]](#)
- [3] Song, Q. N., Wang, Y., Jin, Z. T., Zhang, Y. C., Xu, N., Bao, Y. F., . . . & Zhang, H. L. (2024). Comparison of the corrosion and cavitation erosion behaviors of the cast and surface-modified manganese-aluminum bronzes in sodium chloride solution. *Journal of Materials Research and Technology*, 30, 4310–4321. [\[CrossRef\]](#)
- [4] Cobo Ocejó, I., Biezma Moraleda, M. V., & Linhardt, P. (2022). Corrosion behavior of heat-treated nickel-aluminum bronze and manganese-aluminum bronze in natural waters. *Metals*, 12(3), Article 380. [\[CrossRef\]](#)
- [5] Song, Q. N., Zhang, H. N., Li, H. L., Hong, H., Sun, S. Y., . . . & Qiao, Y. X. (2022). Corrosion and cavitation erosion behaviors of the manganese-aluminum-bronze cladding layer prepared by MIG in 3.5% NaCl solution. *Materials Today Communications*, 31, Article 103566. [\[CrossRef\]](#)
- [6] Cobo, I., Biezma-Moraleda, M. V., & Linhardt, P. (2022). Corrosion evaluation of welded nickel aluminum bronze and manganese aluminum bronze in synthetic sea water. *Materials and Corrosion*, 73(11), 1788–1799. [\[CrossRef\]](#)
- [7] Linhardt, P., Biezma, M. V., Strobl, S., & Haubner, R. (2023). Influence of Cavitation in Seawater on the Etching Attack of Manganese-Aluminum-Bronzes. *Solid State Phenomena*, 341, 25–30. [\[CrossRef\]](#)
- [8] Mota, N. M., Tavares, S. S. M., do Nascimento, A. M., Zeeman, G., & Biezma-Moraleda, M. V. (2021). Failure analysis of a butterfly valve made with nickel aluminum Bronze (NAB) and manganese aluminum Bronze (MAB). *Engineering Failure Analysis*, 129, Article 105732. [\[CrossRef\]](#)
- [9] Lelevic, A., & Walsh, F. C. (2019). Electrodeposition of Ni P alloy coatings: A review. *Surface and Coatings Technology*, 369, 198–220. [\[CrossRef\]](#)
- [10] Liu, C., Yin, Y., Li, C., Xu, M., Li, R., & Chen, Q. (2022). Preparation and properties of Ni-P/Bi self-lubricating composite coating on copper alloys. *Surface and Coatings Technology*, 443, Article 128617. [\[CrossRef\]](#)
- [11] Shajari, Y., Alizadeh, A., Seyedraoufi, Z. S., Razaivi, S. H., & Shamakhi, H. (2019). The effect of heat treatment on wear characteristics of nanostructure Ni-B coating on marine bronze. *Materials Research Express*, 6(10), Article 105040. [\[CrossRef\]](#)
- [12] Sahoo, P., & Das, S. K. (2011). Tribology of electroless nickel coatings – A review. *Materials & Design*, 32(4), 1760–1775. [\[CrossRef\]](#)
- [13] Avcu, E., Abakay, E., Yildiran Avcu, Y., Çalim, E., Gökalp, İ., Iakovakis, E., . . . & Guney, M. (2023). Corrosion behavior of shot-peened Ti6Al4V alloy produced via pressure-assisted sintering. *Coatings*, 13(12), Article 2036. [\[CrossRef\]](#)
- [14] Islam, M., & Shehbaz, T. (2011). Effect of synthesis conditions and post-deposition treatments on composition and structural morphology of medium-phosphorus electroless Ni-P films. *Surface and Coatings Technology*, 205(19), 4397–4400. [\[CrossRef\]](#)
- [15] Alizadeh, M., & Dashtestaninejad, M. K. (2016). Fabrication of manganese-aluminum bronze as a shape memory alloy by accumulative roll bonding process. *Materials & Design*, 111, 263–270. [\[CrossRef\]](#)
- [16] Ashassi-Sorkhabi, H., & Rafizadeh, S. H. (2004). Effect of coating time and heat treatment on structures and corrosion characteristics of electroless Ni-P alloy deposits. *Surface and Coatings Technology*, 176(3), 318–326. [\[CrossRef\]](#)
- [17] Kordijazi, A. (2014). Electrochemical Characteristics of an Optimized Ni-P-Zn Electroless Composite Coating. *Advanced Materials Research*, 1043, 124–128. [\[CrossRef\]](#)